JCB Report

Filamin A, the Arp2/3 complex, and the morphology and function of cortical actin filaments in human melanoma cells

Lisa A. Flanagan, Janet Chou, Hervé Falet, Ralph Neujahr, John H. Hartwig, and Thomas P. Stossel

Hematology Division, Brigham and Women's Hospital, Department of Medicine, Harvard Medical School, Boston, MA 02115

The Arp2/3 complex and filamin A (FLNa) branch actin filaments. To define the role of these actin-binding proteins in cellular actin architecture, we compared the morphology of FLNa-deficient human melanoma (M2) cells and three stable derivatives of these cells expressing normal FLNa concentrations. All the cell lines contain similar amounts of the Arp2/3 complex. Serum addition causes serum-starved M2 cells to extend flat protrusions transiently; thereafter, the protrusions turn into spherical blebs and the cells do not crawl. The short-lived lamellae of M2 cells contain a dense mat of long actin filaments in contrast to a more three-dimensional orthogonal network of shorter actin filaments in lamellae of identically treated FLNa-expressing cells capable of translational locomotion. FLNa-specific antibodies localize throughout the leading lamellae of these cells at junctions between orthogonally intersecting actin filaments. Arp2/3 complex–specific antibodies stain diffusely and label a few, although not the same, actin filament overlap sites as FLNa antibody. We conclude that FLNa is essential in cells that express it for stabilizing orthogonal actin networks suitable for locomotion. Contrary to some proposals, Arp2/3 complex–mediated branching of actin alone is insufficient for establishing an orthogonal actin organization or maintaining mechanical stability at the leading edge.

Introduction

A characteristic actin filament organization exists in the lamellae of spread and translocating cells. Many actin filaments overlap at high angles to one another in X-shaped configurations, or else form T- or Y-shaped end-to-side junctions. This arrangement, often described as orthogonal, fills the spaces between parallel bundles of radially or circumferentially oriented actin filaments (Heuser and Kirschner, 1980; Hartwig and Shevlin, 1986; Lewis and Bridgeman, 1992; Small et al., 1995; Svitkina et al., 1997).

The first actin filament cross-linking protein proposed to induce orthogonal actin filament organization in mammalian cells was filamin A (FLNa),* previously named actin-binding protein or ABP-280. FLNa is the most widely distributed mammalian member of a protein family also expressed in birds and insects with paralogues in lower eukaryotes (for review see Stossel et al., 2001; van der Flier and Sonnenberg, 2001). FLNa efficiently gathers actin filaments into a three-dimensional gel in vitro by cross-linking actin filaments such that the pointed (slow-growing) ends of actin filaments abut the sides of others at high angles (Hartwig et al., 1980; Niederman et al., 1983). FLNa molecules localize specifically to many orthogonal actin filament junctions in cellular cytoskeletons (Hartwig and Shevlin, 1986; Hartwig et al., 1989; Hartwig, 1992; Bailly et al., 1999). However, recent literature discounts FLNa and ascribes a predominant role of making orthogonal actin networks at the leading edge to 70° branching of actin filaments by the Arp2/3 complex (for review see Higgs and Pollard, 2001). Arrays of actin filaments branching at precisely 70° dominate model schemes depicting the leading edge of cells.

An FLNa-deficient human melanoma cell line and derivative rescued sub-lines expressing approximately wild-type FLNa concentrations, afford an opportunity to examine the relative roles of FLNa and the Arp2/3 complex in establishing and maintaining actin filament architecture in the cell periphery. Cultured human melanoma cell lines that do not express FLNa are more easily deformed than other melanoma cell lines that contain FLNa. The FLNa-null cells are unable to migrate across porous filters in response to chemoattractants. Under conditions expected to promote

Address correspondence to Thomas P. Stossel, Hematology Division, Brigham and Women's Hospital, 221 Longwood Ave., LMRC 301, Boston, MA 02115. Tel.: (617) 278-0380. Fax: (617) 734-2248. E-mail: tstossel@rics.bwh.harvard.edu

*Abbreviation used in this paper: FLNa, filamin A.

Key words: actin networks; Arp2/3 complex; cell migration; filamins; blebbing

cell locomotion, the FLNa-deficient cells exhibit continuous circumferential blebbing. Expression of FLNa in one of these cell lines (M2) by transfection with FLNa cDNA yielded sub-lines with decreased deformability that migrated across porous filters with increasing rates in proportion to FLNa expression levels up to the wild-type amount (Cunningham et al., 1992). Although these findings strongly implied that a lack of actin filament cross-linking by FLNa leads to aberrant actin filament organization incapable of maintaining surface stability or supporting locomotion, a direct examination of actin filament architecture in FLNa-deficient cells has been lacking.

Results and discussion

Motility of FLNa-null and -repleted cells

Removal of serum causes M2 cells to cease blebbing after 30 min and to remain quiescent with circumferential flat lamellae ribbed by short filopodia. Within 10 min after the addition of serum, the M2 cells extend a ruffling lamella around the entire cell periphery; however, within hours they revert to blebbing. The M2 cells at the edge of a wounded monolayer also predominantly exhibit bleb formation, but occasionally extend flat, lamellar regions that may have small blebs at the periphery. The lamellar structures do not lead to movement of these cells into the wound space. Therefore, M2 cells can respond to agonists with surface activity, but they cannot translate their response into directed locomotion.

M2 sub-lines expressing FLNa (A5, A7, and B3) display polarized lamellae that actively extend filopodia and ruffles. After serum withdrawal the cells remain asymmetric in shape but stop ruffling. 6–10 min after serum addition the cells resume protrusion with ruffling lamellae. The movement of A5 and A7 cells across porous filters was previously reported (Cunningham et al., 1992), and A7 and B3 cells

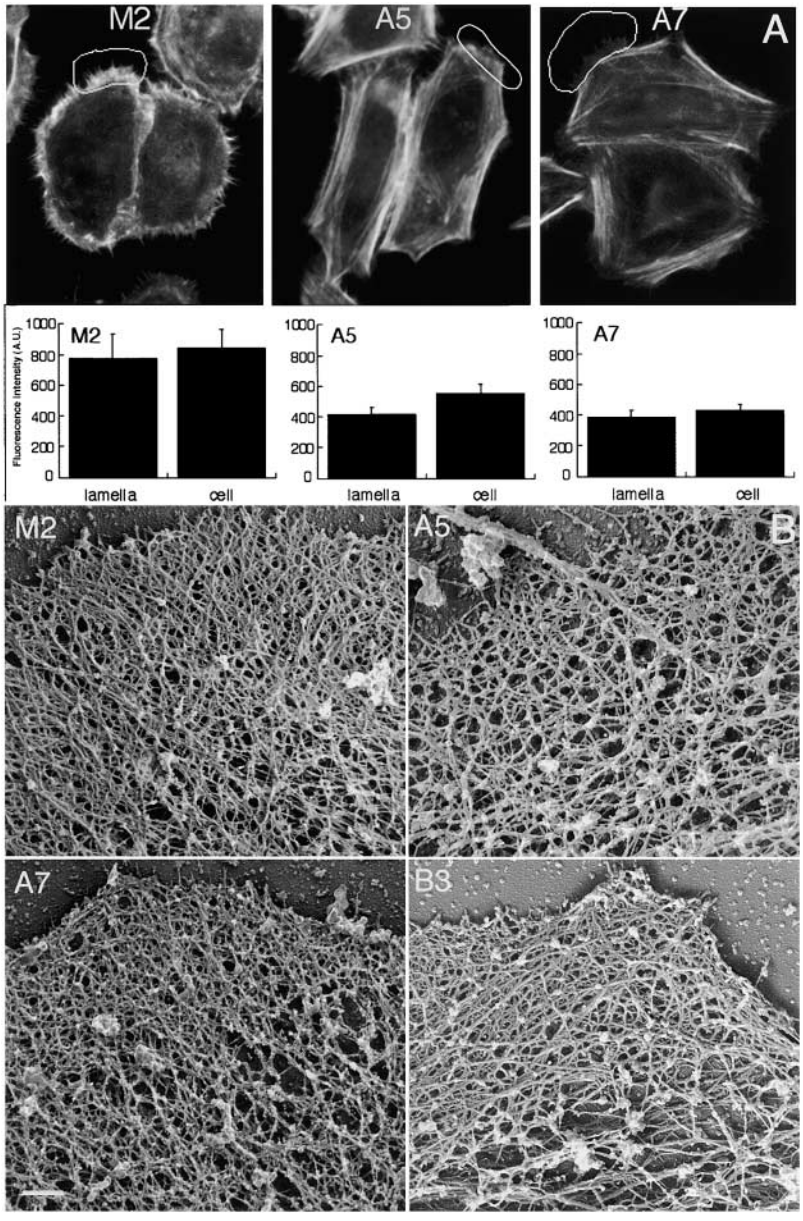

Figure 1. **F-actin content and organization differ in flattened regions of FLNa-null and -repleted cells.** (A) Rhodamine phalloidin staining of M2 cells shows F-actin in lamellae 10 min after serum stimulation. Serum-stimulated A5 and A7 cells show comparatively weaker lamellar F-actin staining and a stronger signal in peripheral linear arrays. The bar graphs summarize quantification of rhodamine phalloidin staining of lamellar regions (highlighted areas in images show representative regions used for analysis) and of whole cells, showing increased F-actin content in serum-stimulated M2 cells relative to serum-stimulated A5 and A7 cells. The values are means ± SEM of measurements on seven or more separate cells. (B). Actin cytoskeletons of lamellar regions of M2, A5, A7, and B3 cells serum stimulated for 10 min and then prepared by quick-freeze, deep-etch electron microscopy. The lamellar regions of M2 cells are wide but thin, whereas similar regions in the other cell lines show more three-dimensional actin filament organizations. Bar, 200 nm.

also close a wound in vitro, moving at an average rate of 20 μm/h.

Increased actin content in lamellar regions of cells lacking FLNa

Serum-starved M2 cells treated with serum for 10 min show F-actin staining in the entire flat, lamellar region that surrounds the cell periphery, and the staining reveals fine projections (Fig. 1 A). Identically treated A5 and A7 cells show linear strands of F-actin staining throughout the cell and around the periphery, as well as F-actin staining in lamellae extended from discrete locations around the cell. A quantitative analysis of F-actin staining reveals that the F-actin content of the lamellar regions of the M2 cells is ~1.8-fold greater than that of A7 or A5 cells. Quantification of the signal over the whole cell shows a similar difference in F-actin content between M2, A7, and A5 cells (Fig. 1 A, bar graphs).

Ultrastructure of M2 and A7 cells

Consistent with the fluorescence analysis of F-actin mass, the density of cortical actin filaments visible in electron micrographs of the broad but thin lamellae extended by M2 cells stimulated with serum for 10 min is higher than that of filaments in the more three-dimensional lamellae that predominate in identically treated A5, B3, or A7 cells (Fig. 1 B). The lamella consists of a dense mat of interwoven filaments oriented mostly perpendicular with a slight offset to the cell edge. Similar structures were observed in flattened regions of M2 cells at wound edges. Occasionally, filaments abut one another and run together before separating. A few radial bundles at the base of filopodia, corresponding to the fine projections seen by fluorescence microscopy, intersperse with overlapping filaments, some of which insert onto the bundles. This filament architecture extends uniformly from the cell edge over a distance of ~4 μm.

The peripheral actin mesh of A5, B3, and A7 cells treated with serum for 10 min is more delicate and three-dimensional than in the M2 lamella. Compared with the M2 cell cortical actin cytoskeleton, the average length of filaments is shorter and the branch angles appear higher. Therefore, the porosity of the actin network is greater in the three-dimensional lamellae of FLNa-repleted cells. These differences in the electron microscopic appearance of actin filaments in lamellae were consistent in 15 sets of specimens examined.

Levels of Arp2/3 are similar in FLNa-null and -reconstituted cells

A polyclonal antibody raised against an epitope unique to FLNa recognizes a 280-kD band on immunoblots of A5, B3, and A7 cell lysates, but shows no reactivity with immunoblots of M2 cell lysates (Fig. 2 A). Fig. 2 A also shows that a polyclonal antibody specific for FLNb detects a high molecular mass polypeptide in lysates from all of the cell lines tested. All of the cell lysates have similar amounts of Arp2/3 complex proteins (Fig. 2 A). A more detailed analysis of M2 and A7 lysates compared with known amounts of Arp2/3 complex show no difference in the levels of Arp2/3 complex proteins between these cells (Fig. 2 B).

Localization of FLNa and the Arp2/3 complex by immunofluorescence in A7 cells in serum

Arp3 immunostaining is diffuse and punctate throughout the cytoplasm of A7 cells in serum (Fig. 2 E). The Arp3 signal intensity increases nearer the nucleus, suggesting a correlation of staining intensity with cytoplasmic volume. The Arp3 antibody also stains the lamellae of these cells. FLNa is

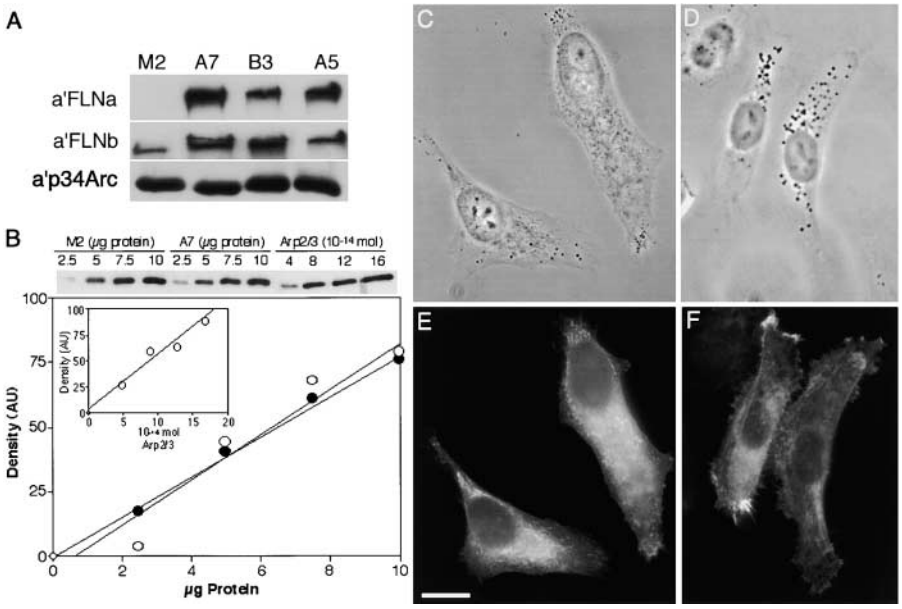

Figure 2. **Levels of Arp2/3 complex and filamin and their immunofluorescent distributions in M2 and derivative cells.** (A) Cell lysates were probed with antibodies that specifically recognize either FLNa, FLNb, or the p34Arc subunit of the Arp2/3 complex. M2 cells have no detectable FLNa signal, whereas the FLNa-transfected cells show strong immunoreactivity for this filamin isoform. All the cells express FLNb, and the lysates show equal reactivity with the p34Arc antibody, regardless of filamin level. Equal amounts of total protein were loaded in each lane and were 20 (FLNa), 40 (FLNb), and 10 μg (p34Arc). (B) Dilutions of purified human platelet Arp2/3 complex and M2 and A7 cell lysates were resolved by SDS-PAGE and immunoblotted with polyclonal antibodies directed against the Arp3 and p34-Arc subunits of the Arp2/3 complex. The experiment shown was obtained with p34-Arc and is representative of the two subunits studied. The graphs display the density of the scanned bands plotted against the amount of purified Arp2/3 complex (inset) or M2 (●) or A7 (○) cell lysates obtained from a single immunoblot. (C–F) A7 cells were stained with antibodies to Arp3 (E) or FLNa (F). Phase contrast images (C and D) are also shown. Both Arp3 (E) and FLNa (F) immunofluorescence signals extend to the edge of lamellar regions of the cells and are detectable in ruffling lamellae. Bar, 5 μm.

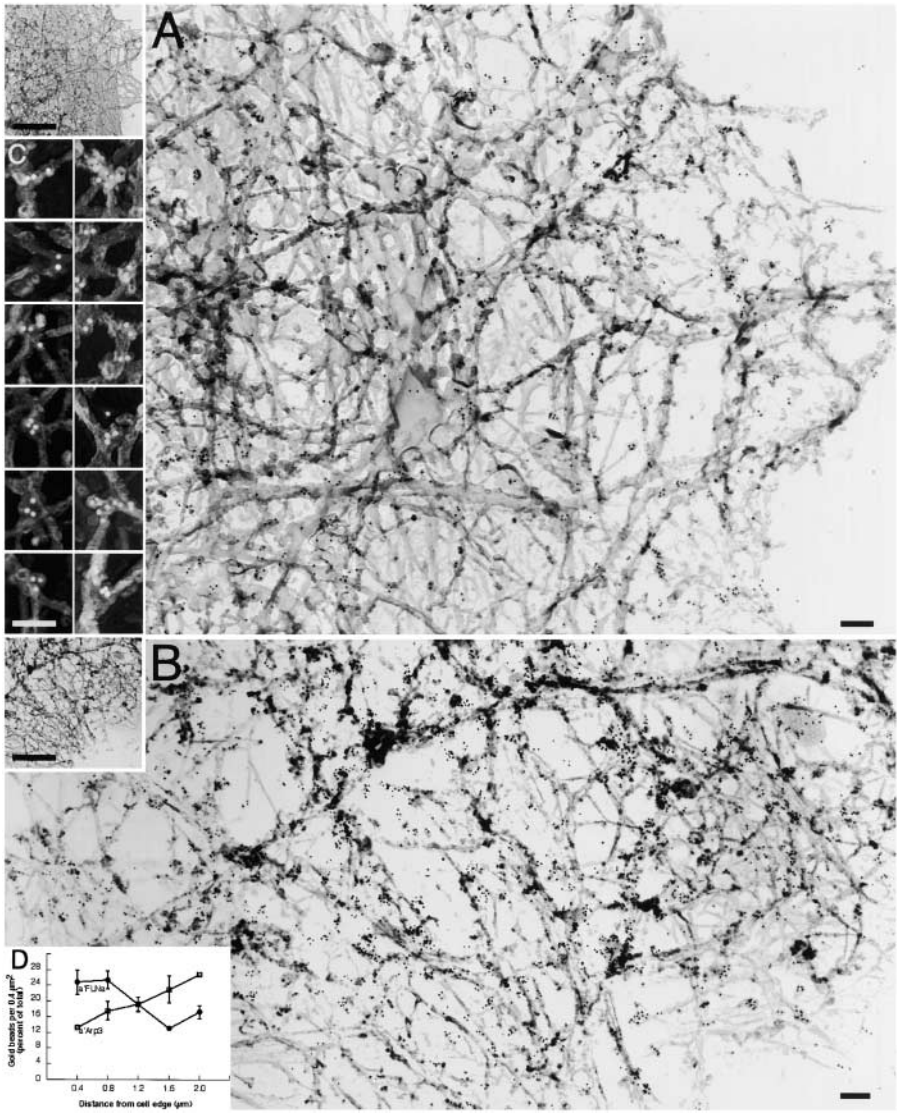

Figure 3. **Immunogold electron microscopic analysis of FLNa and Arp2/3 localization in A7 cell lamellae.** The insets show lower magnification images of cells from which the high-magnification views were taken. Serum-starved A7 cells were treated with serum for 10 min, and then processed for immunogold electron microscopy using polyclonal antibodies to FLNa (A) or Arp3 (B). In B, the specimen was treated with sodium dodecyl sulfate. Both antibodies label actin filaments throughout the lamella right up to the edge of the cell, and the inset (D) displays this information quantitatively. Panel A and inset C reveal that linear clusters of gold localize FLNa at actin filament junctions. Bars: (A and B) 100 nm; (insets, A and B) 1 μm; (inset, C) 100 nm.

diffusely present throughout the cell, but localizes at the periphery of lamellae and with stress fibers that align along the long axis of the cell body (Fig. 2 F). FLNa staining is also detectable at the bases of filopodia as previously reported (Ohta et al., 1999).

Localization of FLNa and the Arp2/3 complex in lamellae of A7 cells by electron microscopy

The ultrastructural analysis of FLNa localization in A7 cells stimulated with serum for 10 min reveals FLNa molecules throughout the periphery of the cell (Fig. 3 A). At 10 min of serum stimulation the majority of the FLNa immunogold signal localizes to the most peripheral 800 nanometers of the lamellae (Fig. 3 D). Higher magnification views of the FLNa staining at 10 min of serum stimulation show extensive colocalization with junctions between actin filaments (Fig. 3 C). The FLNa gold labeling tends to occur in extended clusters, suggesting a reaction of the polyclonal antibodies with multiple sites on the extended FLNa subunits (Gorlin et al., 1990). No staining was observed with secondary antibodies alone, and M2 cells showed no staining with anti-FLNa primary antibodies.

Immunogold staining of the lamellae of serum-stimulated A7 cells for the Arp2/3 complex gives a strong signal, extending to the periphery of the cell (Fig. 3 B). Quantitation of the immunogold signal reveals a somewhat different distribution than that of FLNa. At 10 min of serum stimulation, the Arp2/3 complex signal shows a profile of increasing signal intensity from the periphery back toward the cell body (Fig. 3 D).

The requirement for dodecyl sulfate denaturation of cytoskeletons to expose Arp3 epitopes reactive with available antibodies has hitherto hindered more direct comparisons of their location to those of FLNa, because the denaturation step interferes with binding of many FLNa antibodies, including those used for the experiments described in Fig. 3. We determined that a combination of two monoclonal anti-FLNa antibodies report FLNa in sodium dodecyl sulfate–treated A7 cells by immunofluorescence and immunogold staining and showed no staining in identically prepared M2 cells. These antibodies, generated against human platelet filamin antigen, are specific for FLNa (van der Ven et al., 2000). As expected from the results with separate staining protocols,

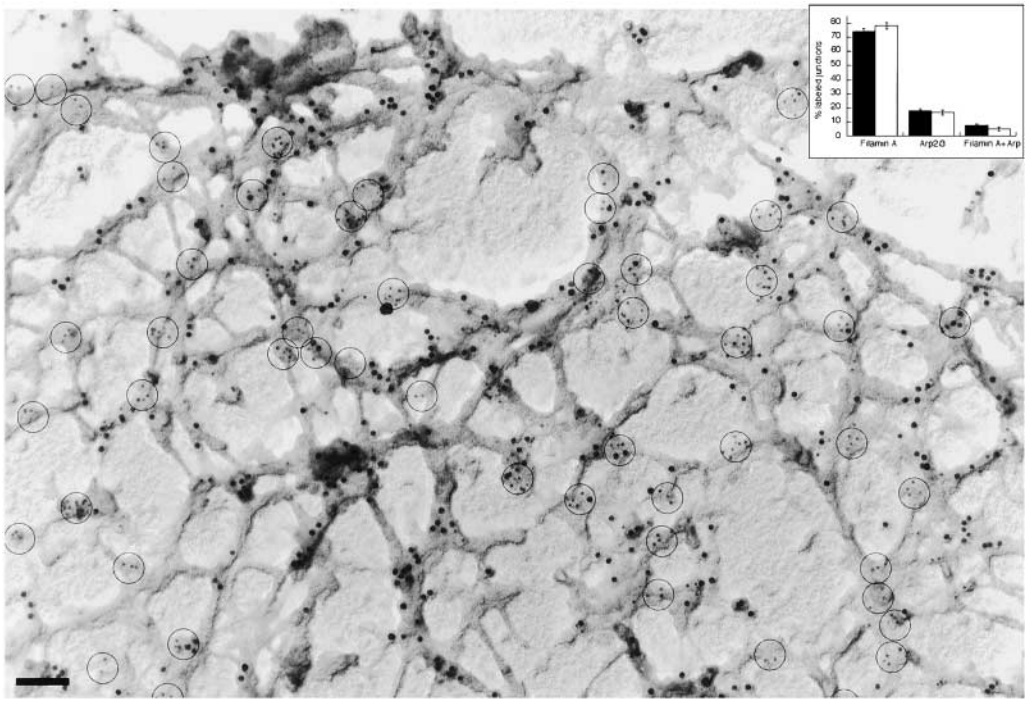

Figure 4. **Double labeling of FLNa and Arp3 in a sodium dodecyl sulfate–treated A7 cytoskeleton.** A7 cells grown in serum were permeabilized, and then labeled with two separate monoclonal antibodies to FLNa (10-nm gold beads) and a polyclonal antibody against Arp3 (5-nm gold beads, highlighted by circles). Both antibodies label actin filament junctions at the cell periphery. Quantitation of the labeled junctions in A7 cells (shaded bars) and B3 cells (unshaded bars) reveals that the FLNa and Arp3 signals rarely overlap and are most often distinct (inset). The values are means ± SEM of measurements on four or more separate cells. Bar, 100 nm.

FLNa and the Arp2/3 complex localize with actin filaments in the periphery of A7 cells (Fig. 4). However, by using gold beads of different sizes, unique aspects of staining are apparent. First, as observed with the polyclonal anti-FLNa antibodies, the monoclonal antibodies often reveal beads lining up more or less in rows at interfilament junctions, consistent with an array along FLNa subunits attached to the sides of filaments near the junctions to hold them in place. Second, Arp3 staining reveals more compact structures, sometimes at filament–filament junctions, but Arp3 and FLNa staining is infrequently visible at the same filament overlap sites. A quantitative analysis of the staining reveals that for both A7 and B3 cells, the majority of the immunolabeled junctions show staining for FLNa alone (inset). Some junctions contain only Arp2/3 complex, and a small minority of junctions are stained with both FLNa and Arp2/3.

In this paper, we have documented that the functional impairment of FLNa-deficient M2 cells is manifest in the presence of normal amounts of the Arp2/3 complex. The lamellae of M2 cells have a very different actin organization from FLNa-repleted cells. The extended lamellae contain increased amounts of filamentous actin, and the actin filaments extend in parallel over long distances, are highly interpenetrated, and form a dense flat mat. In contrast, the periphery of spread FLNa-containing cells contains a much more delicate and orthogonal three-dimensional lattice. Consistent with the importance of an orthogonal web for locomotion, M2 cells do not crawl. To flatten and spread, M2 cells, lacking FLNa, polymerize more actin than FLNa-containing cells, and the higher actin concentrations create a dense meshwork of long filaments presumably strengthened by other actin filament cross-linking proteins.

To protrude the cell surface, an assembled actin lattice must be sufficiently rigid to exert or maintain directionality of the protruding force. A branched structure, like a tree, can be rigid, but in order for a tree to behave as a solid the branches themselves as well as the branch-to-branch joints must be inflexible. Images of unperturbed actin filaments up to a micron or so long can appear straight, but longer filaments bend, and views of actin filaments extending for several microns off of 70°Arp2/3-actin junctions reveal considerable filament curling (Weaver et al., 2001). Because of this flexibility, branched, but not otherwise cross-linked actin filaments, are unable to maintain a rigid structure under stress over the many microns encompassed by a leading lamella. Linking together of branched filaments could provide the requisite elasticity.

Although some 70° actin filament branches are detectable in a dense actin network revealed in cytoskeletons of keratocytes and fibroblasts, such junctions are only readily identified by removing considerable actin filament mass that otherwise obscures these structures (Svitkina and Borisy, 1999). Without such sample preparation, antibody labeling of the Arp2/3 complex has been evident throughout the cell lamellae without defining any particular structures (Bailly et al., 1999; Svitkina and Borisy, 1999). Our results staining M2 and A7 cells are consistent with the earlier findings. Arp2/3 complex staining, done with the same antibody and sample preparation techniques used by previous investigators, was detectable everywhere in the spread lamellae of

M2 and A7 cells, often in aggregates, and at some actin filament junctions.

Filamin molecules have been localizable by immunocytochemistry at actin filament crossover junctions in cortical cytoskeletons, without having to resort to any special actin extraction procedures (Hartwig and Shevlin, 1986; Hartwig et al., 1989; Hartwig, 1992; Bailly et al., 1999). Using two different sample preparation techniques, we have shown here that polyclonal and monoclonal antibodies specific for FLNa label actin filament junctions throughout the lamella up to the plasma membrane of A7 cells. One exception to the otherwise consistent localization of FLNa at peripheral actin filament junctions is a reported failure of immunogold staining of peripheral actin filament junctions in cytoskeletons of human fibroblasts. This experiment used a monoclonal anti-filamin antibody generated in our laboratory, and produced a reaction with a few actin filament junctions far from the plasma membrane (Svitkina and Borisy, 1999). We have also not been able to label cortical actin cytoskeletons with that antibody, and therefore ascribe the negative results reported as purely technical in origin. Residence of FLNa molecules at the cell edge is in accordance with the numerous partnerships between FLNa and plasma membrane proteins (for reviews see Stossel et al., 2001; van der Flier and Sonnenberg, 2001).

FLNa binds many cellular components, including signaling intermediates and membrane receptors, and abnormal functioning of these binding partners is manifest in FLNa-null melanoma cells (Stossel et al., 2001; van der Flier and Sonnenberg, 2001). Although indirect effects of FLNa deficiency based on changes in these interactions are possible, the diminished viscoelasticity and the striking blebbing phenotype of stimulated M2 cells strongly point to an impairment in mechanical stability of the actin filaments underlying the membrane. The ability of FLNa to cross-link actin filaments efficiently in vitro implicates FLNa as an important component for the direct establishment of proper actin filament organization.

The Arp2/3 complex unquestionably causes actin filament branching, but such branching is not sufficient to maintain three-dimensional orthogonal networks. Conversely, FLNa produces orthogonal actin networks in vitro without the intermediacy of Arp2/3 complexes (Hartwig et al., 1980; Niederman et al., 1983). Therefore, the Arp2/3 complex is not a requirement for determining this kind of actin network structure, although it may importantly contribute to the spatial and temporal regulation of that process in vivo (Bailly et al., 2001; Higgs and Pollard, 2001).

Materials and methods

Cell lines and culture conditions

Cell line M2 and M2-derived lines A5 and A7 have been described previously (Cunningham et al., 1992; Cunningham, 1995). Another sub-line, B3 of M2, expressing FLNa under direction of a cytomegalovirus promoter, was a gift of Sue Ann Woo and Dr. John Blenis (Department of Cell Biology, Harvard Medical School, Boston, MA). Cells were grown on glass coverslips coated with poly-D-lysine (0.52 $\mu g/cm^2$) in MEM containing 8% calf serum, 2% fetal calf serum, 10 mM Hepes, pH 7.6, and 0.5 mg/ml G418 (GIBCO BRL). For migration assays, confluent monolayers were wounded with a pipette tip to form gaps of $\sim$ 350 μm, and video microscopy images were collected every 5 min for 16 h. Wound dimensions and cell motility rates were calculated using the NIH Image program.

Antibodies and western blot analysis

Rabbit polyclonal IgG antibodies generated against peptides specific to the first hinge domain of human FLNa (residues 1761–1777) and against the first hinge domain of human FLNb (residues 1717–1733) were affinity purified using the peptide antigens bound to Sepharose 2B. Antibodies were tested for isoform specificity using the same peptides and recombinant FLNa in binding and competition experiments. Two IgG monoclonal anti-FLN antibodies (MAB 1680 and MAB 1678) were purchased from Chemicon, Inc. Anti-FLN IgGs were used at 1:1,000 dilutions for immunoblotting and at 1:100 dilutions for immunofluorescence or immunogold labeling. Rabbit polyclonal antibodies to the Arp3 and p34Arc subunits of the human Arp2/3 complex (Welch et al., 1997) were provided by Dr. Matthew Welch (University of California, Berkeley, CA) and were used at 1:50 dilution for cell staining. The Arp2/3 complex, purified from human platelets by a modification of the method of (Egile et al., 1999), was a gift from Dr. Fumihiko Nakamura (Brigham and Women's Hospital, Boston, MA). Lysates were prepared for immunoblotting by harvesting cells at 80% confluency from 10-cm dishes. Cells were trypsinized, suspended in serum-containing media, centrifuged and washed with PBS to remove serum proteins, and suspended in homogenization buffer (20 mM Tris buffer, pH 7.6, 1 mM EGTA, 0.5 mM $MgSO_4$, 10 μg/ml leupeptin, 5 μg/ml pepstatin A, 10 μg/ml aprotinin, 0.2 mM AEBSF [4-{2-aminoethyl}benzenesulfonyl fluoride]). Cells were homogenized by 20 passes with a small-volume Teflon-on-glass Dounce homogenizer and by two freeze–thaw cycles. Total protein was determined by the Bradford assay calibrated with a BSA standard curve. Varying dilutions of cell lysates or of purified platelet Arp2/3 complex were loaded onto 7.5% (FLNa and FLNb) or 10% (Arp2/3) polyacrylamide gels with a 4% stacking gel for SDS-PAGE. Proteins were electrophoretically transferred onto nitrocellulose paper, and blots were stained with 0.1% wt/vol Ponceau S in 1% acetic acid to verify equal loading and transfer. Ponceau S was removed with sequential rinses of TBS-Tween (50 mM Tris buffer, pH 7.6, 150 mM NaCl, 0.05% Tween 20), and the blots were blocked in 5% nonfat dry milk in TBS-Tween. Antibodies were diluted in 5% nonfat dry milk in TBS (50 mM Tris base, pH 7.6, 150 mM NaCl) and blots were rinsed in TBS-Tween. Primary antibodies were detected with an HRP-conjugated goat anti–rabbit IgG secondary antibody (Promega), and the secondary antibodies detected with an enhanced chemiluminescence system (Pierce Chemical Co.).

Immunofluorescence microscopy

Cells were rinsed with PBS, followed by fixation with 3.7% paraformaldehyde, 5 mM $MgCl_2$, 10 mM EGTA, and 0.1% saponin in PBS for 10 min, rinsed three times in PBS, and then permeabilized with 0.3% Triton X-100 in PBS for 5 min and washed three times with PBS before staining with the polyclonal anti-FLNa antibody. For staining of cells with the polyclonal antibody against Arp3 and the Chemicon monoclonal antibodies against FLNa, cells were fixed with 1% glutaraldehyde in PHEM buffer, pH 6.9 (60 mM Pipes, 25 mM Hepes, 10 mM EGTA, 2 mM $MgCl_2$), with 0.1% saponin for 10 min, washed with PBS, treated with 0.1% sodium dodecyl sulfate in PHEM buffer for 1 min, and rinsed with PHEM buffer. Reactive aldehydes were blocked with 1 mg/ml sodium borohydride in PHEM buffer for 2 min, and removed by washing three times with 0.5% BSA in PBS. Fixed cells were incubated for 1 h at room temperature in blocking solution (5% BSA in PBS). Primary and rhodamine- or fluorescein-labeled anti–rabbit secondary antibodies (Jackson ImmunoResearch Laboratories) were diluted in 1% BSA in PBS and incubated with cells either overnight at 4°C (primary antibody) for 2 h at room temperature (secondary antibody). Phalloidin, either labeled with TRITC or FITC, was included in the secondary antibody incubation at a concentration of 250 nM to label actin filaments according to the phallotoxin product protocol provided by Molecular Probes. Coverslips with stained cells were mounted with Vectashield anti-bleaching media (Vector Laboratories) and viewed on a Nikon Diaphot 300 inverted microscope equipped with epifluorescence. Images were captured with a Micromax cooled CCD camera (1300 × 1030; Roper Scientific) driven by Inovision image processing software on an SGI O_2 computer. Images were processed and compiled using Adobe Photoshop 5.0. NIH Image was used for quantification, and all data were analyzed using the Kaleidagraph program. Pixels were not saturated, and images were taken at the same exposure time so that background intensities were matched. Images were thresholded and selected for analysis using the feature analysis routine, which defined the lamella or whole cell from the background. The output of the selection was compared with the original image to confirm that either the lamella or the entire cell had been selected for analysis. The sum of the intensity of the region was calculated and output to a text file for further analysis.

Electron microscopy

Cytoskeletons were prepared from M2 and A7 cells and processed for

electron microscopy by washing with PHEM, extraction with 0.75% Triton X-100 in PHEM buffer containing 1 μM phalloidin and 0.01% glutaraldehyde for 2 min, and washing with PHEM followed by fixation with 1% glutaraldehyde in PHEM containing 0.1 μM phalloidin for 10 min.

In labeling experiments using the polyclonal anti-Arp3 or monoclonal anti-FLNa antibodies, the cytoskeletons were treated with dodecyl sulfate and unreacted aldehydes blocked as described for immunofluorescence staining. The secondary antibodies were 5- or 10-nm gold-conjugated anti–rabbit or anti–mouse IgGs (Ted Pella).

Gold-labeled cytoskeletons were rapidly frozen on a helium-cooled copper block, freeze dried at −85°C in a Cressington freeze-fracture machine (CFE-50; Ratford), and rotary coated with 1.4 nm of tantalum/tungsten followed by 3 nm of carbon without rotation. Replicas were floated off using 25% hydrofluoric acid, water washed, and collected on 200 mesh copper grids coated with formvar. Grids were photographed in a JEOL 1200-EX electron microscope at 100 kV.

To quantify the immunogold distribution in the lamellae of A7 and B3 cells, rectangular masks of 1 μm × 0.4 μm were laid over images, and all gold beads within the rectangle manually counted (the total area counted in each lamella was 2.4 μm^2).

This reseach was supported by United States Public Health Service grants HL19429 and HL56252, the American Cancer Society, and the Edwin S. Webster Foundation.

Submitted: 31 May 2001
Revised: 27 September 2001
Accepted: 1 October 2001

References

Bailly, M., F. Macaluso, M. Cammer, A. Chan, J. Segall, and J. Condeelis. 1999. Relationship between Arp2/3 complex and barbed the barbed ends of actin filaments at the leading edge of carcinoma cells after epidermal growth factor stimulation. *J. Cell Biol.* 145:331–345.

Bailly, M., I. Ichetovkin, W. Grant, N. Zebda, L. Machesky, J. Segall, and J. Condeelis. 2001. The F-actin side binding activity of the Arp2/3 complex is essential for actin nucleation and lamellipod extension. *Curr. Biol.* 11:620–625.

Cunningham, C. 1995. Actin polymerization and intracellular solvent flow in cell surface blebbing. *J. Cell Biol.* 129:1589–1599.

Cunningham, C., J. Gorlin, D. Kwiatkowski, J. Hartwig, P. Janmey, H. Byers, and T. Stossel. 1992. Actin-binding protein requirement for cortical stability and efficient locomotion. *Science.* 255:325–327.

Egile, C., T. Loisel, V. Laurent, R. Li, D. Pantaloni, P. Sansonetti, and M.-F. Carlier. 1999. Activation of the CDC42 effector N-WASP by the *Shigella flexneri* IcsA protein promotes actin nucleation by Arp2/3 complex and bacterial actin-based motility. *J. Cell Biol.* 146:1319–1332.

Gorlin, J., R. Yamin, S. Egan, M. Stewart, T.P. Stossel, D.J. Kwiatkowski, and J.H. Hartwig. 1990. Human endothelial actin-binding protein (ABP, nonmuscle filamin): a molecular leaf spring. *J. Cell Biol.* 111:1089–1105.

Hartwig, J. 1992. Mechanisms of actin rearrangements mediating platelet activation. *J. Cell Biol.* 118:1421–1442.

Hartwig, J.H., and P. Shevlin. 1986. The architecture of actin filaments and the ultrastructural location of actin-binding protein in the periphery of lung macrophages. *J. Cell Biol.* 103:1007–1020.

Hartwig, J.H., J. Tyler, and T.P. Stossel. 1980. Actin-binding protein promotes the bipolar and perpendicular branching of actin filaments. *J. Cell Biol.* 87: 841–848.

Hartwig, J.H., K.A. Chambers, and T.P. Stossel. 1989. Assocation of gelsolin with actin filaments and cell membranes of macrophages and platelets. *J. Cell Biol.* 108:467–480.

Heuser, J., and M. Kirschner. 1980. Filament organization revealed in platinum replicas of freeze-dried cytoskeletons. *J. Cell Biol.* 86:212–234.

Higgs, H., and T. Pollard. 2001. Regulation of actin filament network formation through Arp2/3 complex: activation by a diverse array of proteins. *Annu. Rev. Biochem*. 70:649–676.

Lewis, A., and P. Bridgeman. 1992. Nerve growth cone lamellipodia contain two populations of actin filaments that differ in organization and polarity. *J. Cell Biol.* 119:1219–1243.

Niederman, R., P. Amrein, and J.H. Hartwig. 1983. The three dimensional structure of actin filaments in solution and an actin gel made with actin-binding protein. *J. Cell Biol.* 96:1400–1413.

Ohta, Y., N. Suzuki, S. Nakamura, J. Hartwig, and T. Stossel. 1999. The small GTPase RalA targets filamin to induce filopodia. *Proc. Natl. Acad. Sci. USA.* 96:2122–2128.

Small, J., M. Herzog, and K. Anderson. 1995. Actin filament organization in the fish keratocyte lamellipodium. *J. Cell Biol.* 129:1275–1286.

Stossel, T., J. Condeelis, L. Cooley, J. Hartwig, A. Noegel, M. Schleicher, and S. Shapiro. 2001. Filamins: integrators of cell mechanics and signaling. *Nat. Rev. Cell Mol. Biol.* 2:138–145.

Svitkina, T., and G. Borisy. 1999. Arp2/3 complex and actin depolymerizing factor/cofilin in dendritic organization and treadmilling of actin filament array in lamellipodia. *J. Cell Biol.* 145:1009–1026.

Svitkina, T., A. Verkhovsky, K. McQuade, and G. Borisy. 1997. Analysis of the actin-myosin II system in fish epidermal keratocytes: mechanism of cell body translocation. *J. Cell Biol.* 139:397–415.

van der Flier, A., and A. Sonnenberg. 2001. Structural and functional aspects of filamins. *Biochim. Biophys. Acta.* 1538:99–117.

van der Ven, P., S. Wiesner, P. Salmikangas, D. Auerbach, M. Himmel, S. Kampa, K. Hayess, D. Pacholsky, A. Taivainen, R. Schröder, O. Carpén, and D. Fürst. 2000. Indications for a novel muscular dystrophy pathway: γ-filamin, the muscle-specific filamin isoform, interacts with myotilin. *J. Cell Biol.* 151: 235–247.

Weaver, A., A. Karkinov, A. Kinley, S. Weed, Y. Li, J. Parsons, and J. Cooper. 2001. Cortactin promotes and stabilizes Arp2/3-induced actin filament network formation. *Curr. Biol.* 11:370–374.

Welch, M., A. DePace, S. Verma, A. Iwamatsu, and T. Mitchison. 1997. The human Arp2/3 complex is composed of evolutionarily conserved subunits and is localized to cellular regions of dynamic actin filament assembly. *J. Cell Biol.* 138:375–384.